



Rail Damage Potentials of Sloshing Cargo

J.A. Romero*, E. Betanzo-Quezada, S.A. Obregón-Biosca

Queretaro Autonomous University, Querétaro, Mexico

ABSTRACT

In this paper a two-degree-of-freedom model representing the sprung mass and the sloshing cargo in a vehicle is proposed to study the dynamic interaction of a sloshing cargo and the carrying vehicle, to simulate the dynamic wheel forces on the rails as a result of lateral perturbations derived from turnings along the railway path and the resultant cargo sloshing. The use of the Fourth- and Third- Power Laws to assess the potential effect of sloshing forces on the life expectancy of rails reveals that differences in rail damage can occur along the rail length, with hot spots suffering as much as 34% more damage than other parts of the rail. It is also found that the damage increases with the square of the speed, and that sloshing damping can reduce the rail damage to one-half when the traveling speed is 70 km/h. Further research is suggested, to validate the model and to take into account rail unevenness.

Keywords: Railways, Sloshing cargo, Contact stresses, Fourth-Power Law, Track geometry

1. Introduction

Contact stresses at the wheel-rail interface cause different forms of rail surface deterioration, including corrugations of different amplitude as a function of axle load [1]: from short to large pitch, which can be severe (1.5 mm) or light (less than 0.1 mm). Shelling is another rail defect caused by wheel loads, which develops in curved portions of the track, some mm underneath the rail surface [1]. Squats are another form of load-related railway defects that occurs at irregular intervals, as a function of the existence of switches and turnouts [2]. In relation with the effect of the magnitude of the axle load on rail deterioration, it has been suggested that it keeps the following relationship [3]:

$$L_{10} = \left(\frac{C}{P}\right)^P \quad (1)$$

where L_{10} is the life for 10% probability of failure, C is the bearing basic dynamic load rating, and P is the

equivalent load on the bearing, with the exponent p in the range of 3 to 4. This equation corresponds to the well-known Fourth Power Law, used to assess the effect of axle loads on pavement condition [4], and according to which an increase of just 10% in tire loads can produce a pavement damage on the order of 46% (1.1^4). In this context, static and dynamic loads sum up to generate wheel-rail loads. While the static part of these forces depend on the cargo distribution on the cars, dynamic components derive from car's vibration as a result of rail unevenness and track geometry, or can originate from the cargo-vehicle interaction in the case of liquid cargo [5]. Inertial forces associated to liquid sloshing are known to affect the lateral stability of vehicles, whether on the road or on the railway, as cargo mobility within its containers generate inertial forces as a result of directional or speed changing maneuvers. In the case of road tankers, studies have shown that the lateral stability of such vehicles can be affected as a result of cargo forces even in the case of high fill levels [6]. In this context, and based upon

* Corresponding Author
 Email Address: jaromero@uaq.mx

experimental results, it has been reported that the sloshing effect on the vehicle lateral stability, measured through the variations of suspension forces on both sides of the vehicle, can represent decreases of lateral stability on the order of 36% [7]. In the case of road transportation, the effect of cargo sloshing has been considered in [8], reporting that the cargo sloshing could influence the road damage potentials of road tankers as a function of not only the fill level of the tank but also as a function of the tank shape. In the case of a cylindrical tank, it is reported that sloshing cargo can increase in 40% the pavement damage in certain road spots.

In the case of railway cars carrying a liquid cargo, only few studies have been reported for analyzing the effect of cargo sloshing on the behavior of tanker cars. Younesian et al. [5] study the effect of cargo sloshing on the derailment potential of trains, reporting an increase of around 20% in derailment probability due to cargo sloshing. They also report increases on the order of 10% in derailment and unloading ratios when the car tank is half-filled, when compared with a fully loaded railway tanker. In a recent paper, Di Gialleoardo et al. [9] report that sloshing can increase in a rather significant manner the rollover trend of the tanker while the risk of derailment being minor. So, while the rollover trend due to sloshing forces could be under discussion in the light of these reported investigations, no discussion would exist regarding the developing of dynamic wheel forces on the rail as a result of cargo sloshing. In this paper, a mathematical model is proposed for simulating the effect of sloshing forces on the magnitude of wheel-rail contact forces, further analyzing the potential consequences of such variations on the level of rail deterioration.

2. Model for the tanke car roll response

Figure 1 illustrates a schematic representation of a multi-body dynamic model representing a spring-supported mass that integrates the bogie, chassis and tank, and a mass of liquid body that oscillates at its first mode around the center of the cylinder. The system can be thus described by two pendulums, as shown in Figure 2.

The resulting two-degree-of-freedom system thus consists of an inverted pendulum, coupled at its top to a simple pendulum. For the derivation of the equations of motion, only small amplitude motions are assumed, leading to have only vertical and horizontal forces. For

the simple pendulum representing the sloshing cargo, the equation of motion is described as follows:

$$\ddot{\phi} = \ddot{\theta} \left(\frac{L_{OA}}{l_p} \right) + a_N \left(\frac{1}{l_p} \right) - \frac{g}{l_p} \phi - \frac{C_\theta}{ml_p^2} \dot{\phi} \tag{2}$$

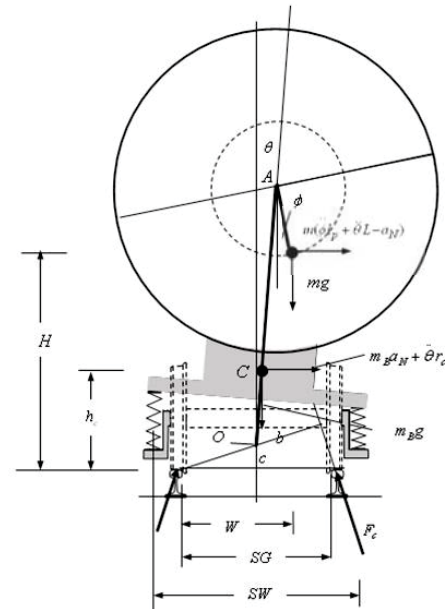


Figure 1: Schematic representation of cargo sloshing in a tanker car subjected to a lateral acceleration (a_N)

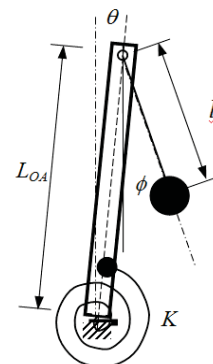


Figure 2: Physical model of the sprung car with a sloshing cargo

which corresponds to a simple pendulum of mass m , whose support is subjected to a lateral acceleration as a result of the oscillating support. a_N in this equation represents the lateral acceleration due to turning maneuvers, g is the gravity acceleration, and C_θ is a damping constant derived from the contact of the fluid with the tank wall.

The corresponding equation for the inverted pendulum results as follows:

$$\ddot{\theta} \left(I_p - r_c^2 m_B - mHL_{OA} \right) = \theta (mgL_{OA} + mgr_c - K) + mgl_p \phi - mHL_p \ddot{\phi} + m_B a_N r_c + ma_N H - C_\theta \dot{\theta} \tag{3}$$

where I_p is the mass moment of inertial of the oscillating tank and bogie chassis, K_θ is the equivalent torsional stiffness associated to the suspension springs, and C_θ is a damping constant. K_θ and C_θ are calculated as a function of the suspension stiffness and damping, k_s and c_s , respectively. The motion of this body is supposed to occur around a roll center, located at the rail level. These equations are manipulated to obtain expressions for $\ddot{\theta}$ and $\ddot{\phi}$. From the diagram of Figure 1, an equation can be obtained for the rail forces by taking force moments around the left rail, as follows:

$$F_c = \begin{pmatrix} \left(m_B \ddot{\theta} r_c \right) h_c + (m_B g) ((SG / 2) + \theta r_c) + \\ m(\ddot{\phi} r_d - \ddot{\theta} L)H + mgW \end{pmatrix} \begin{pmatrix} 1 \\ b \end{pmatrix} \quad (4)$$

where

$$H = c + L_{OA} \cos \theta - r_d \cos \phi = c + L_{OA} - r_d ; r_d = \frac{4r}{3\pi} ;$$

$$h_c = c + r_c \cos \theta ; W = L_{OA} \sin \theta + r_d \sin \phi = L_{OA} \theta + r_d \phi$$

Solution of the equations of motion is obtained through the use of the transition matrix approach [10], according to which the equations of motion can be described as a first order system, as follows:

$$\left\{ \dot{y}(t) \right\} = [A] \{y(t)\} + [B] \{Y(t)\} \quad (5)$$

where

$$\left\{ \dot{y}(t) \right\} = \left\{ \dot{\phi} \quad \ddot{\phi} \quad \dot{\theta} \quad \ddot{\theta} \right\}^T \quad (6)$$

$$\{Y(t)\} = \{0 \quad a_N \quad 0 \quad 0\}^T$$

and

$$[A] = \begin{bmatrix} 0 & 1 & 0 & 0 \\ \pi_1 & \pi_2 & \pi_3 & \pi_4 \\ 0 & 0 & 0 & 1 \\ \pi_5 & \pi_6 & \pi_7 & \pi_8 \end{bmatrix} [B] = \begin{bmatrix} 0 & 0 & 0 & 0 \\ 0 & \mu_1 & 0 & 0 \\ 0 & 0 & 0 & 0 \\ 0 & \mu_2 & 0 & 0 \end{bmatrix} \quad (7)$$

$$\{Y(t)\} = \begin{Bmatrix} 0 \\ a_N \\ 0 \\ 0 \end{Bmatrix}$$

where π 's and μ 's are constants determined by the geometric, stiffness and damping properties of the chassis and cargo. Table 1 lists the values for these geometric, stiffness and damping properties for the system.

3. Performance measure

The effect of dynamic sloshing forces on the railway condition can be assessed through different metrics. However, according to the contact stresses phenomenon involved, the potential damaging effect of wheel forces on the rail should be described through a power-based relationship, such as those used in other contact mechanics phenomena in which a relative increase of, say, 10% in the contact force, represents an increase in the damage around 36% $(1.1)^{3.3}$. For instance, in the case of rolling bearings, its life L can be estimated through the following equation [3]:

$$L = a_1 a_2 a_3 \left(\frac{C}{P} \right)^p \quad (8)$$

where C is the bearing dynamic load rating capacity and P is the equivalent load on the bearing. The exponent p in this equation is 3 for all bearings having an elliptical contact area, 10/3 for ball bearings having a modified line of contact, and 4 for a pure line contact. In this equation, constants a_1 , a_2 and a_3 modify the equation as a function of reliability, material used and operating conditions, respectively.

The shape of the wheel-rail contact patch thus influences any estimation about the effect of rolling forces on the life expectancy of the rails. In this regard, it has been proposed an elliptical contact area in the case of wheel-rail situation [11], so that the exponent p in equation (8) should be 3. However, a similar situation is found in the case of the interface truck tires - pavement, in which the value for such exponent has been proved to be 4 [12][13]. In this context and for swiftly analyze roads subjected to dynamic tire loads, a useful and simplified criterion has been proposed before, which consists of aggregating or summing up the value of the tire forces raised to exponent n , as follows [14]:

$$A_k^n = \sum_{j=1}^{Na} P_{jk}^n \quad (9)$$

where P is the tire force, k represents the position along the road due to the j axle of Na axles of the vehicle. In this work, the potential effect of train wheel forces on the rail condition will be described through this aggregated wheel force raised to the third and fourth powers.

4. Results and discussion

Results are presented for the dynamic response of the resulting mechanical system to variations in lateral

acceleration a_N , which result from turning maneuvers along the rail path. In order to have a first view on the effect of the sloshing damping on the system's response, its free reaction to a speed input is presented in Figure 3. This figure depicts the time histories for the free response of both degrees of freedom to an initial speed imparted to ϕ , for three levels of damping: light, medium and heavy, according to Table 1. These results show different levels of vibration, where the rolling motion of the support is around one tenth that of the sloshing cargo. The effect of sloshing cargo damping will be taken into account later, for assessing the rail damage potentials of the sloshing cargo.

Simulations are now presented concerning the dynamic response of the described model to lateral accelerations associated to the circulation of the train along an actual rail path. Figure 4 describes the existing rail path that will be used to generate the lateral accelerations inputs when such path is run at different speeds by the tanker car. This path is actually run by freight trains and is located around an urban area in a Mexican City. Several turnings of different radius compose this rail path, including a left turn

followed by a right turn, and a close left turn.

Figure 5 illustrates the resultant radius of curvature for the rail path in Figure 4, with radius ranging from 2000 to 229 meters.

Perturbation for the model is obtained by applying the centrifugal force equation, as follows:

$$a_N = v^2 / r \tag{10}$$

where v is the traveling speed and r is the instantaneous radius along the rail path.

For the selected railway path, different sets of simulations are described and analyzed focusing, on the one hand, on the effect of the traveling speed on the level of dispersion of the forces exerted by the wheels on the rails and, on the other hand, on the potential rail damaging effect of such forces for different levels of damping available in the sloshing cargo compartment. Also, a plot is included on the spatial distribution of the damage that would be suffering the rails due to a tanker car loaded at 50% of its capacity. As it was mentioned before, the selected train path includes several changes of direction, which excite the oscillation of the sloshing cargo to the left and right sides. It should be noted that the resulting wheel forces represent the total force on the right side of the wheels of a single tanker car.

Table 1: List of parameters

Property	Value	Property	Value	Property	Value
Gauge length	SG 1.43 m	Arm	b 1.49 m	Roll arm,	L_{OC} 0.7 m
	L_{OA} 2.52 m	Spring constant	k_s 5000000 N/m	Bogie mass	m_B 8 000 kg
Tank radius	r 1.54 m	Spring damping constant	c_s 12000 Ns/m	Distance to roll centre	c 0.23 m
Torsional stiffness constant (4 springs)	K 20000000 Nm/rad	Mass moment of inertia of the bogie and tank	I_p 5000 kg m ²	Tank capacity	113550 litres (30000 gallons)
Torsional damping constant (4 dampers)	1000, 5000 and 3000 Nm s / rad (light, medium and heavy)	Spring width	SW 2.0 m	Liquid mass	m 44 284 kg (gasoline)

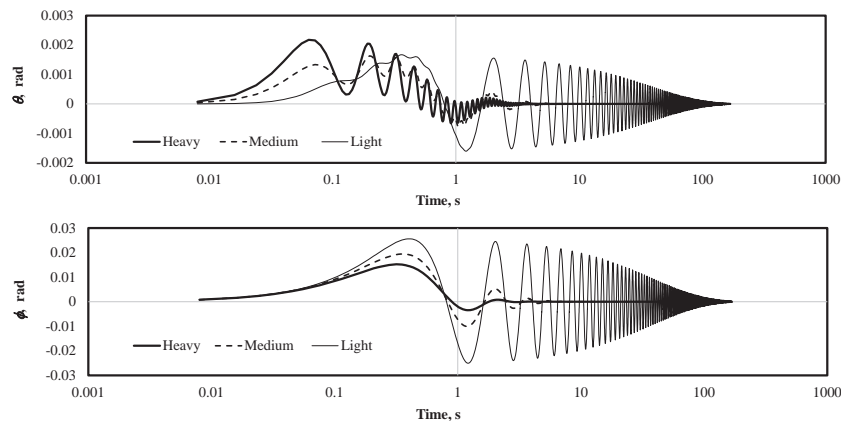


Figure 3: Free response of chassis and sloshing cargo for an initial speed $\dot{\phi} = 0.1$ rad / s

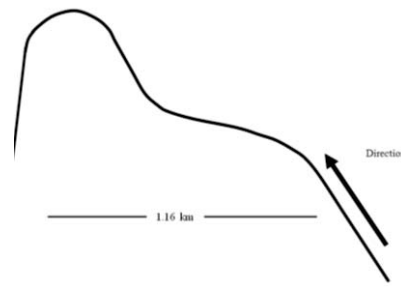


Figure 4: Path of a railway in a Mexican City. (Global coordinates: 200 23' 16.31 N 990 59' 08.85)

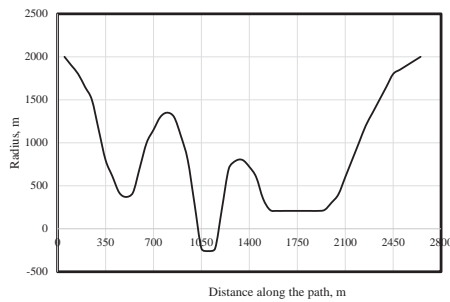
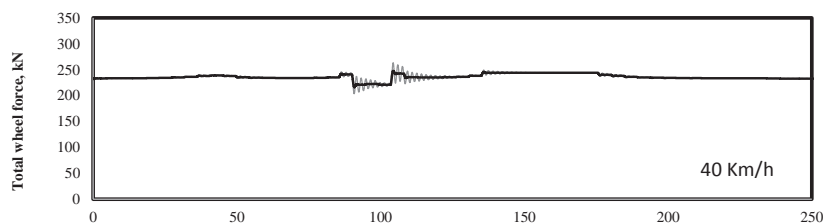


Figure 5: Corresponding radius for the track path in figure 4

Figure 6 illustrates the simulation results of wheel forces for three train speeds, as a function of the sloshing nature of the cargo (sloshing and non-sloshing). For these comparative simulations, the non-sloshing cargo was artificially created through the increase of the available damping, in such a way that the static properties of the cargo remained the same, regardless of the sloshing condition of the cargo. These results reveal that the sloshing cargo generates a dynamic force component around the non-sloshing cargo forces. The amplitude of this oscillation, however, results a function of the train speed, as a higher speed creates a slightly increased oscillation. While for the lowest speed the dynamic increment is around 5%; for the greatest speed considered the sloshing effect represents 20% higher peaks. As it can be observed in these results for the decaying oscillations, the level of damping considered is medium. As the phase angle between the maximum responses between the sloshing and non-sloshing cargoes is minimum, it can be inferred that the variations in the acceleration input due to the selected path followed by the train, do not represent

any dynamic coupling between the acceleration input and tanker car response, as the perturbation frequencies are far lower than the natural responses associated to the coupled liquid-solid body.

It can also be observed in these results that there are portions of the rail that suffer higher forces than others, as a result of the combined result of cargo and vehicle rolling motion. Consequently, the average force for these simulations would tend to be the one corresponding to the non-sloshing cargo, in a potential scenario according to which the damaging effect of the peaks would compensate those of the valleys. However, the potential effect of the wheel forces on the rail condition, according to the selected performance measure, do not depend linearly on the magnitude of the forces, but its relationship obeys a certain power (between three and four). So, the effect of the lower forces do not compensate the effect of the maximum forces. Figure 7 depicts these effects, where a range of variations in the sloshing cargo effect can be simulated according to two different Power Laws and different levels of damping. For generating these data, the instantaneous wheel-rail force was raised to the particular Power-law considered, and then summed up to obtain the global tanker car effect on the full rail length. According to these results, using the Third-Power Law criterion suggests that the maximum effect of the sloshing cargo can vary from 0.72 to 1.75% in the case of the higher speed considered (70 km/h). According to the Fourth-Power Law, however, and for that speed, such an effect vary from 1.9% to 3.55% approximately, as a function of the available sloshing cargo damping.



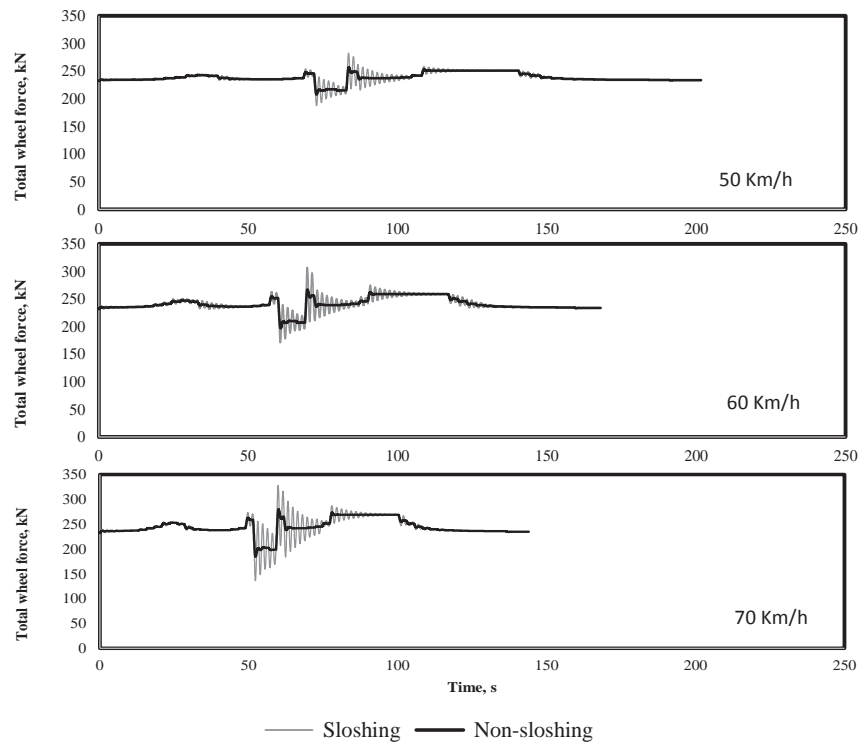


Figure 6: Time histories of wheel-rail total forces on one side of the cargo tanker partially loaded with fuel, at 50% level

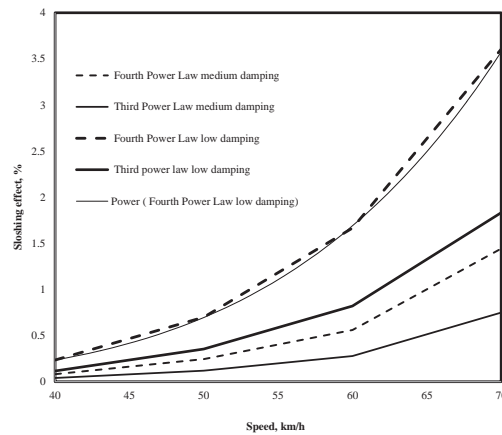


Figure 7: Variation in the potential damaging effect of train wheel forces on rail as a function of damaging law and sloshing cargo damping

On the other hand, it is shown in this Figure 7 that the potential effect of the traveling speed on the rail damage squarely increases with the traveling speed in the case of the Fourth Power Law. As wheel-rail forces variations are the result of the rolling motions of the cargo due to lateral acceleration perturbations imposed by track geometric design that further generate sloshing cargo forces, it can be remarked that tracks geometric design is particularly critical in the case of infrastructures designed for liquid cargo transportation, especially at partial fill levels. By the

way, this situation can also be extrapolated to moving cargoes such as in passenger trains, in particular when carrying standing people. In another extrapolation of these results, the damage of the bogie parts and tanks should also be considered, as the simulated forces are transmitted through the different vehicle components.

With respect to the spatial distribution of rail damage, Figure 8 illustrates the Third and Fourth Power Laws for the lower and higher speeds considered in this study. These results suggest that

the level of damage endured by the rail materials is significant, especially in the case of the Fourth Law criterion. Corresponding ratios of maximum to minimum rail damage in these simulations are presented in Figure 9, as a function of the traveling speed, where values as high as 34 can be reached in the case of the Fourth Power Law at 70 km/h, while in the case of the Third Power Law, the maximum value for this ratio is 14.

5. Conclusions and recommendations

It has been presented a simplified two-degree-of-freedom mathematical model for studying the interaction of an oscillating cargo and the rail transport vehicle, when this vehicle is partially filled with a liquid and travels along a rail path containing left and right turns. While the mathematical model was created through the use of Newton's Second Law, the solution of the linearized equations was obtained through the use of the transition matrix approach. The adoption of a generalized performance measure to assess the rail damage potentials of dynamic bogie wheel forces reveals that sloshing cargo causes concentrations of damage along the rail path, with increases on the order of 34% in the so called hot spots along the railway. While the formulation is based upon basic physical principles, some testing is necessary to validate both the physical model proposed and the rail damage effects due to the dynamic wheel forces. Additionally, another sources of roll perturbations should be incorporated into the model, especially those derived from rail unevenness and natural lateral oscillation of the train cars. Finally, the results presented give a certain perspective regarding the well-known importance of using sloshing suppression devices.

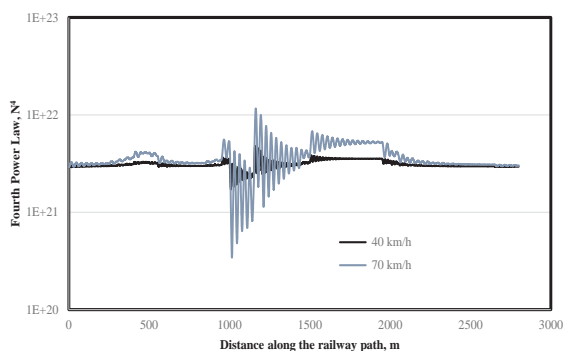


Figure 8: Illustration of the potential position at which the maximum fourth and third power law occurs along the path of train

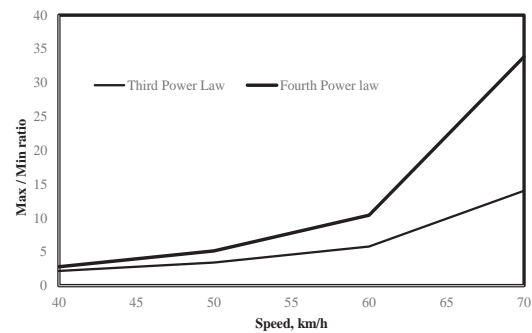


Figure 9: Effect of the speed on the maximum to minimum damage ratios along the rail path, according to the Third- and Fourth Power Laws

6. References

- [1] Engineering manual, Surface defects in rails, TMC 227, Rail Corporation, Asset Standards Authority, New South Wales, Australia, (2013).
- [2] M. Molodova, Z. Li, A. Nunez, R. Dollevoet, Parameter Study of the Axle Box Acceleration at Squats, Proceedings of the Institution of Mechanical Engineers, Part F: Journal of Rail and Rapid Transit, (2014), DOI: 10.1117/0954409714523583.
- [3] F. Sadeghi, N.K. Arakere, B. Jalalahmadi, T.S. Slack, N. Raje, A review of rolling contact fatigue, Journal of Tribology, 131 (2009) DOI: 10.1115/1.3209132.
- [4] N.A. Doodoo, N. Thorpe, A new approach for allocating pavement damage between heavy goods vehicles for road-user charging, Transport Policy, 12 (2005) 419-430.
- [5] D. Younesian, M. Abedi, I. Hazrati Ashtiani, Dynamic analysis of a partially filled tanker train travelling on a curved track, International Journal of Heavy Vehicle Systems, 17 (2010) 331-358.
- [6] J. Romero, O. Ramírez, J. Fortanell, M. Martínez, A. Lozano, Analysis of lateral sloshing forces within road containers with high fill levels, Proceedings of the Institution of Mechanical Engineers, Part D: Journal of Automobile Engineering, 220 (2006) 303-312.
- [7] J. Romero, M. Martinez, E. Betanzo, Experimental study on sloshing and non-sloshing road cargoes dynamics, International Journal of Heavy Vehicle Systems, 17 (2010) 301-330.

- [8] J. Romero, C. López-Cajún, E. Betanzo, M. Arroyo, Road tankers instabilities due to cargo sloshing, Proceedings of Ibero-American Congress on Mechanical Engineering. La Plata, Argentine, (2013).
- [9] E. Di Gialleonardo, A. Premoli, S. Gallazzi, S. Bruni, Sloshing effects and running safety in railway freight vehicles, *Vehicle System Dynamics*, 51 (2013) 1640-1654.
- [10] L. Meirovitch, *Fundamentals of vibrations*. 2001, International Edition, McGraw-Hill.
- [11] W. Yan, F. Fischer, Applicability of the Hertz contact theory to rail-wheel contact problems, *Archive of applied mechanics*, 70 (2000) 255-268.
- [12] N. Sathaye, A. Horvath, S. Madanat, Unintended impacts of increased truck loads on pavement supply-chain emissions, *Transportation Research Part A: Policy and Practice*, 44 (2010) 1-15.
- [13] M. Isola, G. Betti, A. Marradi, G. Tebaldi, Evaluation of cement treated mixtures with high percentage of reclaimed asphalt pavement, *Construction and Building Materials*, 48 (2013) 238-247.
- [14] D. Cole, D. Cebon, Assessing the road-damaging potential of heavy vehicles, *Proceedings of the Institution of Mechanical Engineers, Part D: Journal of Automobile Engineering*, 205 (1991) 223-232.